

Fast Li diffusion in crystalline LiBH_4 due to reduced dimensionality: Frequency-dependent NMR spectroscopy

V. Epp and M. Wilkening*

Institute of Physical Chemistry and Electrochemistry, Gottfried Wilhelm Leibniz University Hannover, Callinstr. 3a, D-30167 Hannover, Germany

(Received 13 May 2010; published 16 July 2010)

The hexagonal and orthorhombic form of lithium borohydride, LiBH_4 , are investigated by temperature and frequency-dependent nuclear magnetic resonance (NMR) spectroscopy. The local electronic structure and microscopic diffusion parameters are determined by recording both $^6,7\text{Li}$ NMR spectra and spin-lattice relaxation (SLR) rates. The rates of the high-temperature flank of the SLR-NMR peaks of hexagonal LiBH_4 clearly depend on resonance frequency which unequivocally reveals a low-dimensional diffusion process. Due to the very limited number of suitable model substances this makes lithium borohydride an extremely attractive material to study the effect of reduced dimensionality on Li dynamics. Most likely, the spatial confinement of Li hopping is also responsible for the very high ionic conductivity found for the hexagonal polymorph, recently.

DOI: 10.1103/PhysRevB.82.020301

PACS number(s): 66.30.-h, 76.60.-k, 82.47.Aa

Introduction. The hexagonal modification of crystalline lithium borohydride, LiBH_4 , belongs to one of the fastest Li ion conductors discovered¹ with promising application possibilities as electrolyte in all-solid-state rechargeable batteries.²⁻⁴ Materials with high ionic conductivity are highly required for the development of so-called clean energy storage systems which are indispensable when the problem of global warming has to be addressed. In order to meet these challenges, materials science has to focus on the knowledge-based identification of new as well as on the target-oriented improvement of known ion conductors. Certainly, this includes the detailed, atomic-scale investigation of diffusion pathways giving information about the general rules leading to fast ion conduction in solids. In many studies⁵ structural properties such as disorder and defects are discussed to be responsible for enhanced diffusivity. However, the influence of dimensionality is hardly considered to explain transport properties of solids, so far.

Although LiBH_4 is a long-known reducing agent in organic synthesis and considered as an advantageous material for hydrogen storage, the high ionic conductivity of its hexagonal polymorph and modified forms has been found only recently.^{1,6,7} Matsuo *et al.* suggested that Li diffusion is confined to two dimensions (2D) in LiBH_4 .¹ This conclusion is based on a rough comparison of Li jump rates deduced from temperature-variable Li nuclear magnetic resonance (NMR) spin-lattice-relaxation (SLR) measurements with results from electrical impedance spectroscopy. However, such a comparison is fraught with a lot of difficulties since rigorous assumptions concerning correlation factors and the conversion of SLR-NMR rates (T_1^{-1}) into reliable cation jump rates have to be made. Moreover, low-temperature SLR NMR and conductivity measurements probe diffusion and transport parameters, respectively, on quite different length scales. In general, the analysis of diffusion-controlled SLR-NMR rates as a function of the inverse temperature ($1/T$), only, is by far not sufficient to unequivocally find out whether Li migration in LiBH_4 is restricted to two dimensions or not. Instead, frequency-dependent SLR-NMR measurements have to be carried out for this purpose. To our

knowledge, only few such solid-state NMR studies exist so far^{8,9} including an elegant ^1H NMR study by McDowell *et al.*¹⁰ on the metal hydride $\text{ZrBe}_2\text{H}_{1.4}$.

While NMR, when applied to both liquids and solids, offers a large set of techniques widely used to probe diffusion parameters on quite different time and length scales,¹¹⁻¹⁴ it is far less known that recording SLR-NMR rates as a function of resonance frequency $\omega_0/2\pi$ can be employed in a unique way to determine the dimensionality of a given diffusion process from an atomic-scale point of view. Fortunately, randomly oriented powder samples are sufficient for such measurements since the method is solely based on the different spectral density functions $J(\omega)$ controlling diffusion in one dimension, two dimensions, or three dimensions (3D).⁵ In

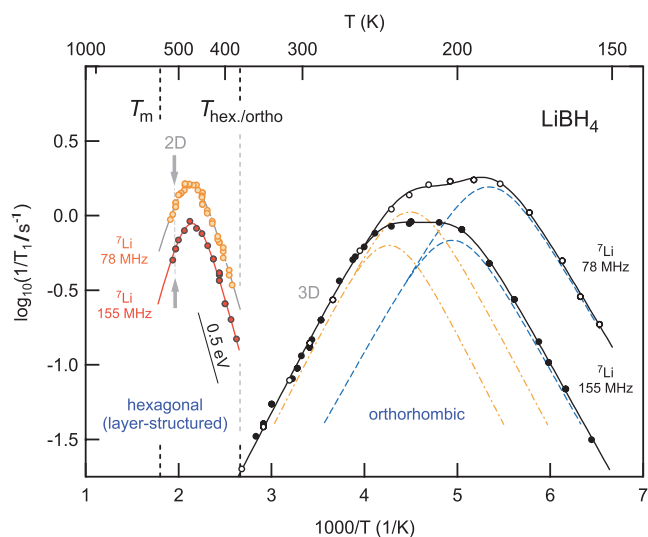


FIG. 1. (Color) Purely diffusion-induced ^7Li SLR-NMR rates of hexagonal and orthorhombic LiBH_4 . The rates were measured at the radio frequencies $\omega_0/2\pi$ indicated. Solid lines in the T range of hexagonal LiBH_4 are to guide the eye. Note the nonvanishing frequency dependence at temperatures above the peak maxima (see arrows) of hexagonal LiBH_4 stable at $T > T_{\text{hex./ortho}}$. See text for further explanations.

the present Rapid Communication we will show that besides its application-oriented relevance, hexagonal LiBH_4 turned out to be one of the very rare materials highly suitable to study the influence of dimensionality on purely diffusion-induced Li SLR-NMR rates. Without any doubt, the frequency dependence of the high-temperature SLR-NMR rates observed here, unequivocally points to a low-dimensional diffusion process in layer-structured LiBH_4 which might also be the key to understand the very high ion conductivity observed, recently.

Experiment. The crystal structure of LiBH_4 was studied by Soulié *et al.*¹⁵ using synchrotron x-ray powder diffraction. Below $T_{\text{hex./ortho}}=381$ K lithium borohydride shows orthorhombic symmetry (space group $Pnma$). At temperatures higher than $T_{\text{hex./ortho}}$ it undergoes a first-order phase transition and becomes hexagonal ($P6_3mc$). The process is fully reversible. LiBH_4 melts at about $T_m=553$ K. Because of this we have restricted our NMR measurements to temperatures lower than 515 K.

Nominally pure LiBH_4 (colorless crystallites with diameters in the micrometer range) was purchased from Alfa Aesar, strictly handled under inert-gas atmosphere and fire sealed in quartz tubes for the NMR measurements. ^6Li and ^7Li SLR-NMR rates were recorded using two Bruker spectrometers (MSL 100 and MSL 400) connected to Oxford cryomagnets of 4.9 T and 9.4 T (shimmed magnet), respectively. The saturation recovery pulse sequence⁵ was used to measure the diffusion-induced recovery of the longitudinal magnetization M as a function of waiting time t after perturbing the equilibrium state, $M(t)=M_0$, with a comb of several closely spaced $\pi/2$ radio-frequency pulses. The corresponding transients $M(t)$, which were measured at different temperatures, strictly follow single exponential time behavior $M(t)=M_0[1-\exp(-t/T_1)]$. NMR spectra were obtained by Fourier transformation of the free induction decays recorded after excitation the sample with a single radio-frequency pulse.

Results and discussion. Before analyzing the SLR-NMR data of hexagonal LiBH_4 it is worth discussing a few details of $T_1^{-1}=f(\omega_0, T)$ of its orthorhombic form where the ^7Li NMR T_1^{-1} rates are indirectly controlled by rapid rotational motions of the BH_4 tetrahedra rather than by fast translational Li jumps.¹⁶ Temperature-variable ^7Li SLR-NMR rates (T_1^{-1}) of orthorhombic LiBH_4 , which were recorded at two different frequencies $\omega_0/2\pi$ (155 and 78 MHz), are shown in Fig. 1.

$T_1^{-1}(1/T)$ can be fitted with a sum (solid lines) of two rate peaks $T_{1,i}^{-1}(\omega_0, T) \propto J_i^{3D}(\omega_0, T) \propto \tau_{c,i}/[1+(\omega_0\tau_{c,i})^2]$ ($i=1, 2$), respectively. They incorporate exponential lattice correlation functions $G_i(t)$, i.e., Lorentzian-shaped spectral density functions $J_i^{3D}(\omega_0)$ as assumed by Bloembergen, Purcell, and Pound (BPP) for 3D random jump diffusion.¹⁷ Note that $J(\omega)$ is the Fourier transform of $G(t)$. The fits $T_{1,i}^{-1}(\omega_0, T)$ were restricted to a single term for a good approximation. The motional correlation time τ_c is given by the Arrhenius relation $\tau_{c,i}=\tau_{c0,i} \times \exp[E_{a,i}/(k_B T)]$ where $\tau_{c0,i}$ represent the pre-exponential factors, $E_{a,i}$ the activation energies, and k_B Boltzmann's constant, respectively. Dashed and dashed-dotted lines in Fig. 1 show the deconvolution of $T_1^{-1}(1/T)$ into the rate peaks $T_{1,1}^{-1}(\omega_0, T)$ and $T_{1,2}^{-1}(\omega_0, T)$, respectively,

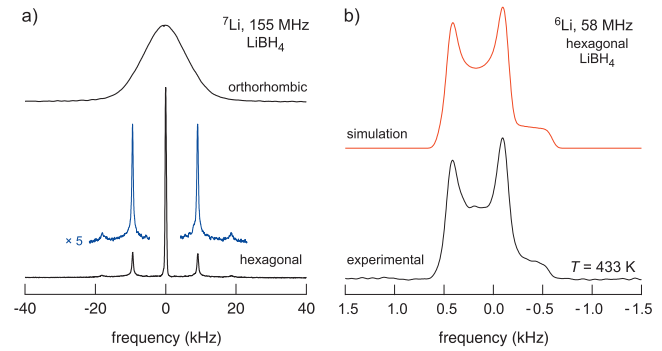


FIG. 2. (Color) (a) ^7Li NMR spectra of orthorhombic (top) and hexagonal LiBH_4 (bottom) recorded at $\omega_0/2\pi=155$ MHz on a nonrotating sample. (b) Static ^6Li NMR spectrum (referenced to a 1 M LiCl) of hexagonal LiBH_4 (bottom) and its simulation using $\delta_q(^6\text{Li})=770$ Hz and $|\Delta\sigma|=3$ ppm, respectively. See text for further explanations.

depending on $\omega_0/2\pi$ each. The activation energies turned out to be $E_{a,1}=0.23(1)$ eV and $E_{a,2}=0.21(1)$ eV. As expected for 3D diffusion the SLR-NMR rate is independent of frequency in the high- T limit $\omega_0\tau_c \ll 1$. At low temperatures, i.e., in the limit $\omega_0\tau_c \gg 1$, a frequency dependence shows up. In this regime T_1^{-1} follows the BPP-type power law $T_1^{-1} \propto \omega_0^{-2}$ for uncorrelated motion which is already implemented in the above-mentioned spectral density function.

As mentioned above, Li SLR-NMR rates reflect the dynamics of the BH_4 units. The fact that Li diffusion is slow in orthorhombic LiBH_4 can be easily verified when ^7Li NMR line shapes are regarded (Fig. 2). In the orthorhombic phase the ^7Li NMR spectrum recorded under static conditions is Gaussian shaped and the corresponding line width (full width at half height), which is approximately 16.5 kHz (see Fig. 2 of an NMR spectrum of the so-called rigid lattice regime which is in perfect agreement to those shown by Corey *et al.*¹⁸), does not change significantly from 155 K up to 380 K. We refer to Ref. 19 for ^7Li magic angle spinning (MAS) NMR spectra which were used to extract information on local electronic structures in ortho- LiBH_4 . Therefore, τ_c is expected to be larger than 1 ms in this T regime rather than on the order of 1 ns as can be estimated from the maxima positions of the $T_{1,i}^{-1}(\omega_0, T)$ rate peaks where $\omega_0\tau_{c,i} \approx 1$ holds. The two rate maxima observed can be attributed to two different rotational jump processes of the BH_4 units which was rationalized by, e.g., ^{11}B and ^1H SLR-NMR measurements, recently.¹⁶

However, the situation of extremely slow Li motions in the orthorhombic form changes dramatically when the structure of LiBH_4 turns into the layered one with hexagonal symmetry. In Fig. 2 the ^7Li NMR spectrum of layer-structured LiBH_4 is compared with that of the orthorhombic form. Above 381 K very similar and fully motionally narrowed NMR spectra are obtained indicating very fast Li diffusion with a mean motional correlation time being much smaller than 0.1 ms. In Refs. 1 and 18 similar observations were made. As expected for a spin-3/2 nucleus such as ^7Li , a well-defined quadrupole powder pattern shows up in this T range revealing distinct inner singularities and outer wings

from which the quadrupole coupling constant $\delta_q(^7\text{Li})$ can be determined. $\delta_q(^7\text{Li})$ turns out to be about 37.06(2) kHz which is in good agreement with results obtained when ^7Li MAS NMR spectra are analyzed.¹⁹ $\delta_q(^7\text{Li})$ characterizes the strength of the electric interaction of the ^7Li quadrupole moment q with the electric field gradient (EFG) produced by the electric charge distribution in the neighborhood of the Li site. The EFG is found to be almost axially symmetric here so that it can be deduced from the quadrupole singularities in a straightforward way²⁰ without invoking a simulation of the spectrum. In principle, this is also possible for the ^6Li NMR spectrum recorded. However, due to the much smaller quadrupole moment of ^6Li compared to ^7Li the relative influence of chemical shift anisotropy $\Delta\sigma$ on the line shape is much larger. Hence, we have simulated the spectrum shown in Fig. 2(b) to determine both $\delta_q(^6\text{Li})$ and $|\Delta\sigma|$ using the program WSOLIDS.²¹ Once again the EFG turned out to be almost axially symmetric and $\delta_q(^6\text{Li})$ and $|\Delta\sigma|$ amount to be about 770 Hz and 3 ppm, respectively. Thus, the ratio $\delta_q(^6\text{Li})/\delta_q(^7\text{Li})=q(^6\text{Li})/q(^7\text{Li})$ is about 0.02, which is in good agreement with a previously reported value obtained in the same way on an Li₃N single crystal.²²

The observed chemical-shift anisotropy as well as the fact that the quadrupole interactions are not averaged by rapid Li hopping on the hexagonal lattice point to a highly anisotropic Li diffusion process. Its low-dimensional nature can be unequivocally verified when the high-temperature flanks ($\omega_0\tau_c \ll 1$) of the corresponding Li NMR $T_1^{-1}(1/T)$ rate peaks recorded at different $\omega_0/2\pi$ values are regarded (Figs. 1 and 3). In the high- T limit a characteristic frequency dependence shows up which can only be interpreted in terms of Li diffusion taking place in confined dimensions. As mentioned above, in the case of 3D diffusion no such frequency dependence shows up in this limit. Note that the high- T flank of a SLR-NMR rate peak is solely influenced by the dimensionality of the diffusion process. This is in contrast to the slope of the low- T flank which can be additionally affected by correlation effects such as Coulomb interactions and/or structural disorder.^{5,23–25} Usually this leads to a reduced slope in the limit $\omega_0\tau_c \gg 1$ resulting in a subquadratic dependence $T_1^{-1} \propto \omega_0^{-\beta}$ with $1 < \beta \leq 2$.⁵ Quite recently, Solonin *et al.* reported on ^7Li NMR relaxation rates in the limit $\omega_0\tau_c \ll 1$; however, they did not analyze their data with respect to dimensionality effects.²⁶

Relaxation models developed for 2D diffusion of dipolarly coupled spins predict a logarithmic frequency dependence of T_1^{-1} on the high- T side of the rate peak.²⁷ The spectral density function $J^{2D}(\omega_0, \tau_c) \propto \tau_c \ln[1 + 1/(\omega_0\tau_c)^2]$ introduced by Richards combines the two limiting cases for low and high temperatures of a 2D system.²⁸ For uncorrelated 2D motion the rate peak is expected to be asymmetric in shape exhibiting a slightly reduced slope in the limit $\omega_0\tau_c \ll 1$ compared to that of the low- T side. In the case of ^7Li SLR NMR this might be masked due to the larger homonuclear and heteronuclear couplings of the ^7Li spins so that an almost symmetric rate peak is observed (see Fig. 1). Note that also in hexagonal LiBH₄ the BH₄ units are expected to perform fast rotational motions. Interestingly, the special characteristics of $J^{2D}(\omega_0, \tau_c)$ can be observed in the case of ^6Li subjected to much smaller coupling mechanisms. In the

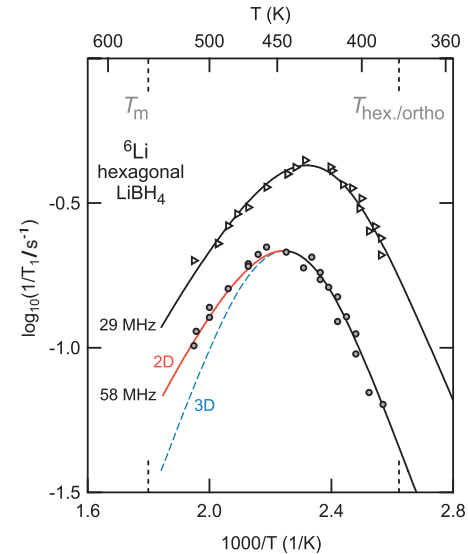


FIG. 3. (Color) Arrhenius representation of the ^6Li SLR-NMR rates of hexagonal LiBH₄ recorded at $\omega_0/2\pi=58$ MHz and 29 MHz, respectively. Solid lines represent fits according to a spectral density function $J^{2D}(\omega_0, T)$ proposed for 2D diffusion (see text) revealing the characteristic asymmetry of the rate peaks $T_1^{-1}(1/T)$. The slope on the high- T flank of the rate peaks is by about a factor of 3/4 smaller than that of the low- T side. Symmetric rate peaks would be obtained in the case of 3D diffusion (indicated by the dashed line).

present study a sample with natural abundance (7.5% ^6Li) was investigated. Therefore, interfering interactions are additionally largely reduced due to the spatial separation of the ^6Li spins (quasispin-1/2 nuclei). In contrast to ^7Li NMR, the smaller frequencies of the ^6Li SLR-NMR measurements allow the detection of larger ranges of the high- T flanks of the rate peaks (see Fig. 3) which shift to lower T when $\omega_0/2\pi$ is decreased. Solid lines in Fig. 3 show fits according to Richards' spectral density function $J^{2D}(\omega_0, \tau_c)$ based on $T_1^{-1}(\omega_0, \tau_c) \propto \tau_c \ln(1/\omega_0\tau_c)$ for $\omega_0\tau_c \ll 1$ and a BPP-type frequency dependence $T_1^{-1}(\omega_0, \tau_c) \propto \omega_0^{-2}\tau_c^{-1}$ for $\omega_0\tau_c \gg 1$ (vide supra). It is worth mentioning that in the case of LiBH₄ the recorded SLR-NMR rates are purely induced by diffusion. Any nondiffusive background effects, see, e.g., Ref. 14, are completely absent, i.e., no correction procedures are necessary to obtain reliable Li T_1^{-1} rates. From the fits shown in Fig. 3 a pre-exponential factor τ_{c0} on the order of 10^{-15} s is obtained being in agreement with values typically found for phonon frequencies. The activation energy turns out to be $E_a=0.54(2)$ eV and characterizes long-range Li diffusion in LiBH₄. It is in good agreement with that deduced from electrical impedance spectroscopy (0.53 eV), recently.¹

Let us note that the same values for E_a and τ_{c0} are obtained when the four-parameter spectral density function is used which was proposed by MacDonald *et al.*²⁹ for like-spin magnetic dipolar interactions between spins undergoing 2D diffusion. In the temperature range covered here the corresponding fits are very similar to those shown in Fig. 3. Analyzing just the rates on the low- T flank of the $^6,7\text{Li}$ SLR-NMR rate peaks leads to $E_a \approx 0.5$ eV as well. In the limit $\omega_0\tau_c \gg 1$ the T_1^{-1} rates are sensitive to localized motions. This

indicates that no difference between short-range and long-range motions in LiBH_4 can be observed by NMR. The same result has been found for layer-structured Li_xTiS_2 , recently.^{11,14}

A singular $T_1^{-1}(1/T)$ rate peak recorded at one resonance frequency only, restricts the possibilities to extract information about the dimensionality of ion dynamics solely to the analysis of the shape of the peak. This necessarily requires highly precise measurements certainly carried out over a large temperature range in order to reveal the small differences between the two slopes on either sides of the maximum, see, e.g., Ref. 14. Even more, an exact model is needed being capable to predict $T_1^{-1}(1/T)$ with respect to structural details of the material under investigation. Let us note that the observed asymmetry highlighted in Fig. 3 might not be observed if the low- T side of the peak is influenced by correlation effects ($\beta < 2$). In such cases symmetric rate peaks may show up masking the information about dimensionality effects in the limit $\omega_0\tau_c \ll 1$. Therefore, frequency-dependent SLR-NMR measurements are by far the best choice to confirm low-dimensional diffusion. The nonvanishing frequency dependence of the T_1^{-1} rates in the limit $\omega_0\tau_c \ll 1$ (see Figs. 1 and 3) also shows up when SLR-NMR rates $T_{10}^{-1}(1/T)$ are recorded in the rotating frame of reference. Preliminary, $T_{10}^{-1}(1/T)$ NMR measurements have been performed at three locking frequencies $\omega_1/2\pi$ ranging from 4.5 to 18 kHz. The data are consistent with a linear dependence of $T_{10}^{-1}(1/T)$ on $\ln(1/\omega_1)$.

Conclusion and outlook. Interestingly, layered-structured Li ion conductors such as Li_3N ,^{30,31} Li containing β'' alumina,³² Li_xCoO_2 ,³³ Li_xMoO_3 ,^{34,35} or Li_xTiS_2 ,¹⁴ for which (dominating) 2D diffusion is already proved or strongly anticipated, often exhibit a high Li diffusivity. Together with the results presented here one might recall the assumption that materials providing diffusion pathways with confined dimensions, i.e., where the mobile ions are guided by structural restrictions, are beneficial for fast diffusion of small cations such as Li^+ . Of course, this might not hold for one-dimensional ionic motion which can be easily blocked by a small concentration of crystal imperfections or impurities. Let us note that Matsuo *et al.* successfully stabilized the hexagonal structure of LiBH_4 down to 340 K by adding binary halides such as LiI ,⁶ see also Ref. 19. Certainly, more investigations are needed in order to develop further rules being helpful in the design of new materials as well as in the controlled manipulation of their diffusion parameters.

We gratefully acknowledge P. Heitjans for many fruitful discussions and for access to the NMR equipment in Hannover. We thank A. Düvel and J. Heine for their technical help. Financial support by the Leibniz University Hannover (Wege in die Forschung II, Dynamo) as well as the Deutsche Forschungsgemeinschaft [research unit 1277 (molife), Grants No. WI 3600 2-1 and No. WI 3600 4-1] is highly acknowledged.

*Author to whom correspondence should be addressed; wilkening@pci.uni-hannover.de; www.wilkening.pci.uni-hannover.de

¹M. Matsuo, Y. Nakamori, S.-i. Orimo, H. Maekawa, and H. Takamura, *Appl. Phys. Lett.* **91**, 224103 (2007).

²J. M. Tarascon and M. Armand, *Nature (London)* **414**, 359 (2001).

³M. S. Whittingham, *Chem. Rev.* **104**, 4271 (2004).

⁴P. Novák, K. Müller, K. Santhanam, and O. Haas, *Chem. Rev.* **97**, 207 (1997).

⁵P. Heitjans, A. Schirmer, and S. Indris, in *Diffusion in Condensed Matter—Methods, Materials, Models*, 2nd ed., edited by P. Heitjans and J. Kärger (Springer, Berlin, 2005), Chap. 9, pp. 369–415.

⁶H. Maekawa *et al.*, *J. Am. Chem. Soc.* **131**, 894 (2009).

⁷M. Matsuo *et al.*, *J. Am. Chem. Soc.* **131**, 16389 (2009).

⁸W. Küchler, P. Heitjans, A. Payer, and R. Schöllhorn, *Solid State Ionics* **70-71**, 434 (1994).

⁹K. Metcalfe *et al.*, *Solid State Ionics* **26**, 209 (1988).

¹⁰A. F. McDowell, C. F. Mendelsohn, M. S. Conradi, R. C. Bowman, and A. J. Maeland, *Phys. Rev. B* **51**, 6336 (1995).

¹¹M. Wilkening, W. Küchler, and P. Heitjans, *Phys. Rev. Lett.* **97**, 065901 (2006).

¹²M. Wilkening *et al.*, *Phys. Chem. Chem. Phys.* **9**, 6199 (2007).

¹³M. Wilkening, A. Kuhn, and P. Heitjans, *Phys. Rev. B* **78**, 054303 (2008).

¹⁴M. Wilkening and P. Heitjans, *Phys. Rev. B* **77**, 024311 (2008).

¹⁵J. Soulié, G. Renaudin, R. Černý, and K. Yvon, *J. Alloys Compd.* **346**, 200 (2002).

¹⁶A. V. Skripov, A. V. Soloninin, Y. Filinchuk, and D. Chernyshov,

J. Phys. Chem. C **112**, 18701 (2008).

¹⁷N. Bloembergen, E. M. Purcell, and R. V. Pound, *Phys. Rev.* **73**, 679 (1948).

¹⁸R. L. Corey *et al.*, *J. Phys. Chem. C* **112**, 18706 (2008).

¹⁹L. M. Arnbjerg *et al.*, *Chem. Mater.* **21**, 5772 (2009).

²⁰T. Bredow, P. Heitjans, and M. Wilkening, *Phys. Rev. B* **70**, 115111 (2004).

²¹K. Eichele, WSOLIDS 1 (2009), Solid-State NMR Spectrum Simulation, Version 1.19.15, University of Tübingen.

²²M. Wilkening, D. Gebauer, and P. Heitjans, *J. Phys.: Condens. Matter* **20**, 022201 (2008).

²³M. Meyer, P. Maass, and A. Bunde, *Phys. Rev. Lett.* **71**, 573 (1993).

²⁴K. Funke, *Prog. Solid State Chem.* **22**, 111 (1993).

²⁵K. L. Ngai, *Comments Solid State Phys.* **9**, 141 (1980).

²⁶A. V. Soloninin, A. V. Skripov, A. L. Buzlukov, and A. P. Stepanov, *J. Solid State Chem.* **182**, 2357 (2009).

²⁷A. Avogadro and M. Villa, *J. Chem. Phys.* **66**, 2359 (1977).

²⁸P. M. Richards, *Solid State Commun.* **25**, 1019 (1978).

²⁹D. H. MacDonald *et al.*, *J. Phys.: Condens. Matter* **10**, 417 (1998).

³⁰D. Brinkmann, M. Mali, J. Roos, R. Messer, and H. Birli, *Phys. Rev. B* **26**, 4810 (1982).

³¹B. Bader *et al.*, *J. Phys.: Condens. Matter* **4**, 4779 (1992).

³²G. C. Farrington and J. L. Briant, *Science* **204**, 1371 (1979).

³³A. Van der Ven, G. Ceder, M. Asta, and P. D. Tepesch, *Phys. Rev. B* **64**, 184307 (2001).

³⁴C. Julien and G. Nazri, *Solid State Ionics* **68**, 111 (1994).

³⁵T. Brezesinski, J. Wang, S. H. Tolbert, and B. Dunn, *Nature Mater.* **9**, 146 (2010).